

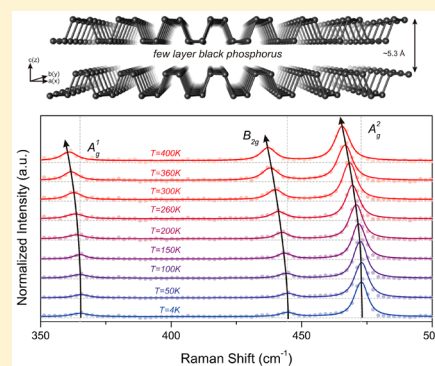
Temperature Evolution of Phonon Properties in Few-Layer Black Phosphorus

Anna Łapińska,^{||} Andrzej Taube,^{§,||} Jaroslaw Judek, and Mariusz Zdrojek^{*}

Faculty of Physics, Warsaw University of Technology, Koszykowa 75, 00-662 Warsaw, Poland

Supporting Information

ABSTRACT: We present the results of Raman measurements of few-layer black phosphorus in a temperature range between 4 and 400 K. The BP Raman mode positions, widths, and intensity ratios exhibit apparent nonlinear temperature dependences, which we attributed to the phenomenon of optical phonon decay into two or three acoustic phonons. These results pave the way for a deeper understanding of the phonon and thermal properties of black phosphorus.



INTRODUCTION

The recently rediscovered^{1,2} black phosphorus (BP) is the newest member of the two-dimensional atomic crystal family.³ Black phosphorus is characterized by many interesting and unique properties⁴ that distinguish it from other two-dimensional materials such as graphene or transition metal dichalcogenides (TMDCs). Black phosphorus is a direct band gap semiconductor both in bulk and in its monolayer form. The band gap of BP decreases with an increase in the number of layers, from approximately 1.45 eV for a monolayer to approximately 0.3 eV for bulk.¹ Black phosphorus is characterized by a very high hole mobility compared with TMDCs that can theoretically² reach $26 \times 10^3 \text{ cm}^2/(\text{V s})$. Experimentally derived mobilities of up to $1300 \text{ cm}^2/(\text{V s})$ at room temperature were demonstrated in high-quality BP flakes sandwiched between hexagonal boron nitride sheets.⁵ At low temperatures, the mobility becomes even larger, thus enabling the observation of quantum oscillations.^{5,6} The high mobility and finite band gap allow the fabrication of high-quality transistors with large $I_{\text{on}}/I_{\text{off}}$ ratios of up to 10^5 and radio frequency operation with a maximum oscillation f_{max} and cutoff f_t frequency of 12 and 20 GHz after de-embedding,^{7–10} respectively. It thus seems that BP is the missing link between graphene and the TMDCs family.¹ Moreover, as a result of its puckered orthorhombic structure (Figure 1a), BP is distinguished by the unique in-plane anisotropy of its optical,^{2,11,12} thermal,^{13–15} and electrical properties.^{2,16–18} These introduce the possibility of the fabrication of new devices with novel functionality.¹⁹

To characterize nanomaterials for various applications, Raman spectroscopy is used as a reliable and nondestructive method.^{20–23} For instance, the temperature-dependent Raman measurements can be used as a tool to investigate vibration,

transport, phonon–phonon properties, or electron–phonon interactions.^{24,25} In the case of BP, the angular dependence of the Raman spectrum can be used as a simple tool for the determination of the crystalline orientation of the investigated flake.¹¹ The Raman optothermal method,²⁶ in which the temperature dependence of the Raman mode position is used, was applied to determine the thermal conductivity of the suspended BP flake.¹³

There have been several studies on the temperature dependence of the Raman spectra of black phosphorus.^{13,14,27} Most of the studies, however, considered only temperatures above 300 K. In those studies, only linear changes of the Raman mode positions with temperature were observed.

Here, we present the evolution of the Raman spectrum of few-layer BP in an extended temperature range from 4 to 400 K. We observe and describe, for the first time, the nonlinear temperature dependence of the BP Raman mode positions, which we attribute to optical phonon decay. In contrast to other works, we also present the effect of the temperature on the Raman mode width and intensity ratios. Our findings are important for further studies on the phonon and thermal properties of black phosphorus and novel devices made of it.

EXPERIMENTAL SECTION

Figure 1a shows a perspective view of the crystalline structure of black phosphorus. The puckered BP single layer consists of two phosphorus atomic planes, in which each phosphorus atom is bound to three adjacent atoms. Subsequent layers are bound to each other by weak van der Waals interactions. The distance

Received: February 11, 2016

Revised: February 14, 2016

Published: February 17, 2016

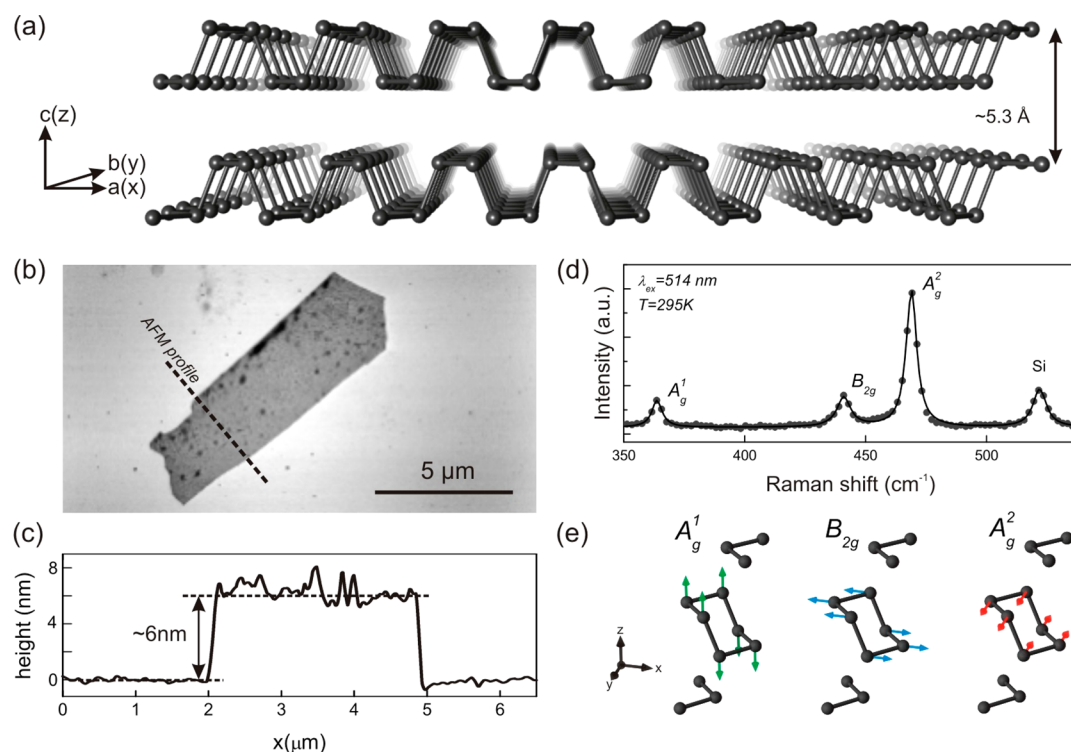


Figure 1. (a) Crystal structure of black phosphorus, (b) AFM image of the investigated few-layer black phosphorus flake, (c) corresponding AFM height profile, (d) room temperature Raman spectrum of few-layer black phosphorus on SiO₂/Si substrate, and (e) atomic displacements of three observed main Raman modes.

between phosphorus atoms in consecutive single layers is approximately 5.3 Å¹. Few-layer BP flakes were fabricated on a SiO₂ (275 nm)/Si substrate by a conventional mechanical exfoliation technique^{28,29} from bulk single crystal (Smart Elements). Particular attention was given to the time when the flakes were exposed to the air because BP is known to be a highly environmentally susceptible material. Recent works have shown the time-dependent instability of the BP flakes caused by water, oxygen, and light flux, which results in partial oxidation to P_xO_y at the BP surface.^{30,31} It was also demonstrated that degradation proceeds only if the black phosphorus is exposed to the above factors simultaneously³⁰ and that the instability of the black phosphorus flake is thickness dependent; that is, the thinner the sample is, the faster the degradation process will proceed.

There is no evidence of degradation if the BP is exposed to oxygen and water in the dark, and exposure to a high photon flux or to oxygen or water (separately) does not result in surface degradation if the BP is placed in a vacuum. To avoid the degradation process, the pristine sample could be placed in a vacuum or passivated by other materials. Thus, after cleaving, the flakes were immediately inspected using optical microscopy and atomic force microscopy (AFM). Then, the samples were transferred to a microscope cryostat and maintained under vacuum. The total time between cleaving and putting the sample under vacuum was <30 min. An AFM image of the investigated BP flake is depicted in Figure 1b. The thickness of the investigated flake, as determined from the AFM image, was approximately 6 nm (Figure 1c). This corresponds to ~9–10 phosphorene layers, considering a possible adsorbate interfacial layer between the flake and the SiO₂/Si substrate. The AFM image also shows no sign of BP flake degradation, and visible small spots are probably the effect of tape residues.

The unpolarized Raman spectra were collected using an Ar laser 514 nm line and a long working distance 50× objective in backscattering geometry. The laser power, calibrated on the sample, was <0.2 mW to avoid excessive sample heating. Temperature-dependent measurements were carried out under vacuum by heating and cooling the sample in a liquid helium cooled microscope cryostat, with the temperature controlled between 4 and 400 K (temperature stability was approximately 0.1 K). To minimize the statistical error, the measurements were performed several times at each temperature point and in different places on the flake. Raman mode parameters were obtained from the Lorentzian fit to the experimental data using the Levenberg–Marquand algorithm (see the [Supporting Information](#) for details of error estimation).

In addition, the same measurements were also performed on thicker (~9.5 nm, see [Figure S1](#)) flakes from the same sample.

RESULTS AND DISCUSSION

Figure 1d shows the room temperature Raman spectra of the investigated few-layer black phosphorus on a SiO₂/Si substrate. According to group theory, there are 12 phonon modes in BP (D_{2h}¹⁸ space group^{11,32}): six Raman-active modes (2A_g, B_{1g}, B_{2g}, and 2B_{3g}), five IR-active modes (2B_{1u}, 2B_{1u} and B_{3u}), and one silent mode (A_u).²⁵ In the backscattering measurement geometry, three main Raman modes are observed: A_{1g}¹, B_{2g}, and A_{2g}² at ca. 363, 440, and 468 cm⁻¹, respectively. Figure 1e presents the atomic displacements corresponding to the observed Raman modes. The A_{1g}¹ mode results from the out-of-plane vibration of phosphorus atoms along the *c*-axis. The B_{2g} and A_{2g}² modes result from the in-plane vibration of phosphorus atoms along the *b*-axis (armchair) and *a*-axis (zigzag), respectively.

Figure 2 shows the normalized Raman spectra of few-layer BP flake taken at selected temperatures. As shown, the

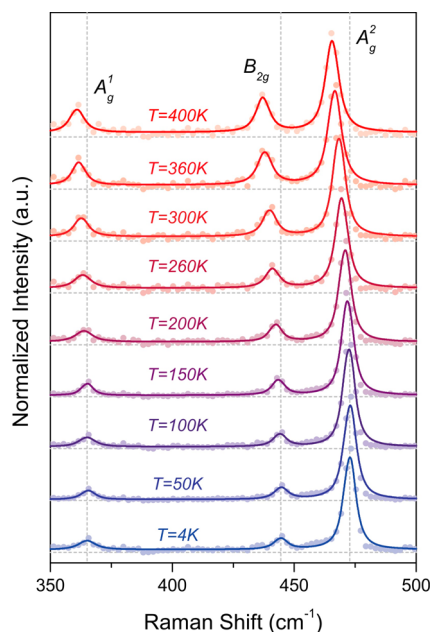


Figure 2. Selected normalized Raman spectra of few-layer black phosphorus measured in the temperature range of 4–400 K.

positions of the Raman modes tend to saturate in the low-temperature range. In contrast, in the high-temperature range, increasing the temperature causes decreases in the Raman mode positions. The detailed temperature dependence of the Raman modes is depicted in Figure 3.

The A_{2g}^2 and B_{2g} modes are shifted by about 7.3 and 7.4 cm^{-1} , respectively, and the A_{1g}^1 mode is shifted by about 4.35 cm^{-1} for

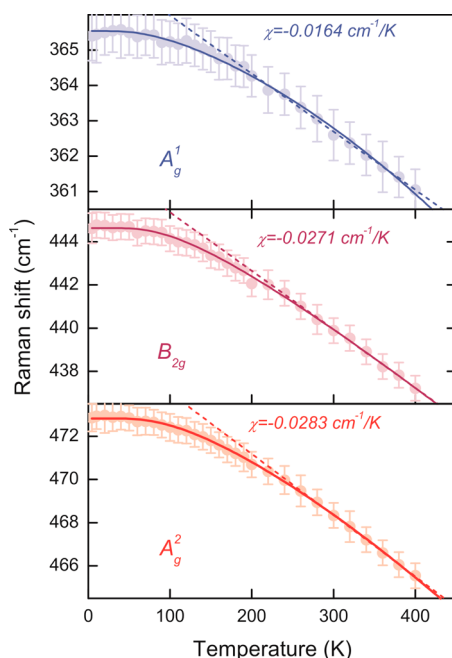


Figure 3. Temperature dependence of black phosphorus Raman mode positions in 4–400 K range. The solid line represents a fit to eq 2, and the dotted line corresponds to a fit to eq 1 (calculated for the 250–400 K temperature range).

temperature change from 4 to 400 K. Generally, the temperature dependence of Raman modes position is related to the electron–phonon, anharmonic phonon–phonon interactions, or thermal expansion.²⁴ The temperature dependence of the Raman mode positions is often described by a first-order temperature coefficient according to the equation^{33–35}

$$\omega(T) = \omega_0 + \chi T \quad (1)$$

where ω_0 is the phonon frequency at a temperature interpolated to 0 K and χ is the first-order temperature coefficient. In our case, this relationship can be applied only for data above 250 K.

The calculated first-order temperature coefficients χ for each of the modes, along with the reported literature values, are presented in Table 1. The χ values are -0.0164 , -0.0271 , and $-0.0283 \text{ cm}^{-1}/\text{K}$ for the A_{1g}^1 , B_{2g} , and A_{2g}^2 modes, respectively. The obtained χ values of the in-plane modes are higher than those of the out-of-plane mode of few-layer BP. The obtained values are in good agreement with the other reported values listed in Table 1. The small differences between our results and those from other groups may be due to different sample preparation procedures or different thicknesses of BP flake, as noted in the footnote in Table 1. Similar results were obtained for thicker ($\sim 9.5 \text{ nm}$) flake (see Table S1). The χ values for BP are much larger than those of other two-dimensional and layered materials such as graphene ($\chi = -0.016 \text{ cm}^{-1}/\text{K}$ for G mode²⁴) and MoS_2 monolayers ($\chi = -0.013$ and $-0.017 \text{ cm}^{-1}/\text{K}$ for A_{1g}^1 and E_{12g} modes³⁶).

Below 250 K, the strong nonlinearity of all Raman mode positions as a function of temperature is apparent, and the linear description is no longer valid.

A much better description of $\omega(T)$ in the whole temperature range can be obtained using the approach developed by Balkanski et al.³⁷ This approach is based on the phenomenon of optical phonon decay into two (three-phonon process) or three (four-phonon process) acoustic phonons with equal energies, stemming from the cubic and quartic anharmonicity of the lattice potential. Thus, the temperature dependence of the Raman mode positions can be described by the relationship

$$\omega(T) = \omega_0 + A \left(1 + \frac{2}{e^x - 1} \right) + B \left(1 + \frac{2}{e^y - 1} + \frac{3}{(e^y - 1)^2} \right) \quad (2)$$

where $x = \hbar\omega_0/2k_bT$, $y = \hbar\omega_0/3k_bT$, ω_0 is the phonon frequency at $T = 0 \text{ K}$, \hbar is the Planck constant divided by 2π , k_b is the Boltzmann constant, and A and B are anharmonic constants. The fit of eq 2 to the Raman mode positions taken from experimental data is presented in Figure 3. Calculated values of the anharmonic constants are presented in Table 2. As shown, the ratio of the constants A/B is high, due to the much larger probability of occurrence of optical phonon decay into two acoustic phonons than into three acoustic phonons. At high temperatures, taking only the first terms of the Taylor expansion, eq 2 tends to a linear dependence, similar to eq 1. A similar nonlinear temperature dependence of Raman mode positions was also observed for other 2D materials such as MoS_2 monolayers³⁸ and ReSe_2 and SnSe_2 nanosheets.³⁹ In addition, nonlinear temperature dependence of Raman mode position was also observed for $\sim 9.5 \text{ nm}$ thick flake (see Figure S2) and the values of the anharmonic constants were similar (at

Table 1. First-Order Temperature Coefficients of Few-Layer Black Phosphorus Raman Modes

mode	χ (cm ⁻¹ /K)		
	A _g ¹	B _{2g}	A _g ²
this work ^a	-0.0164 ± 0.0003	-0.0271 ± 0.0005	-0.0283 ± 0.0004
this work ^b	-0.0172 ± 0.0002	-0.0281 ± 0.0002	-0.0276 ± 0.0006
ref 14 ^c	-0.008	-0.013	-0.014
ref 27 ^d	-0.023	-0.018	-0.023
ref 13 ^e	-0.01895	-0.02434	-0.02316
ref 13 ^f	-0.02175	-0.02877	-0.027

^aCalculated for 250–400 K temperature range, thickness ~6 nm. ^bCalculated for 250–400 K temperature range, thickness ~9.5 nm. ^cSiO₂/Si supported, thickness 4 nm, 77–673 K temperature range ^dSiO₂/Si supported, thickness 5L (~3.2 nm), 113–293 K temperature range ^eSuspended, thickness 9.5 nm, armchair polarization, 296–345 K temperature range ^fSuspended, thickness 9.5 nm, zigzag polarization, 296–345 K temperature range

Table 2. Values of Anharmonic Constants Obtained from the Temperature-Dependence Analysis of Raman Mode Positions

mode	ω_0 (cm ⁻¹)	A (cm ⁻¹)	B (cm ⁻¹)
A _g ¹	366.5 ± 0.18	-0.81 ± 0.2	-0.188 ± 0.03
B _{2g}	448.9 ± 0.17	-4.21 ± 0.4	-0.06 ± 0.02
A _g ²	476.4 ± 0.25	-3.26 ± 0.28	-0.28 ± 0.05

least an order of magnitude, see Table S2) to the values for ~6 nm thick flake.

In addition, we analyzed the effect of temperature on the mode width (full width at half-maximum, fwhm). We observed that the fwhm of the A_g² mode was apparently affected by temperature (Figure 4a) and increases from about 4.92 cm⁻¹ at

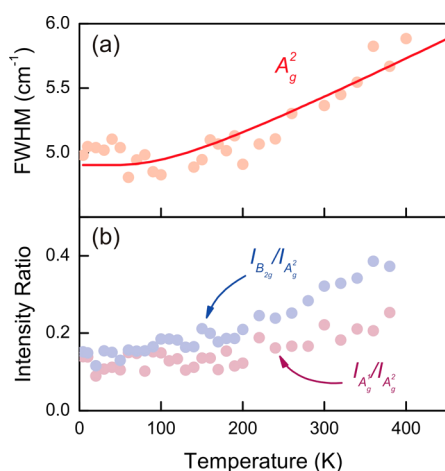


Figure 4. Temperature dependence of (a) black phosphorus A_g² Raman mode width (solid line represents fit to eq 3) and (b) Raman mode intensity ratio in the 4–400 K range. The error of determination of fwhm of A_g² was about ~0.5 cm⁻¹ and of determination of intensity ratios was about ~0.025.

4 K to about 5.88 cm⁻¹ at 400 K. As shown, the A_g² mode width exhibits nonlinear temperature dependence, that is, remains almost constant at low temperatures, and then increases with the temperature above approximately 150 K. The broadening of the Raman mode width, as in the case of the Raman mode position softening, is related to the decay of optical phonon into acoustic phonons and can be described by using the modified approach developed by Balkanski et al.^{37,40}

$$\Gamma(T) = C + \Gamma_0 \left(1 + \frac{2}{e^x - 1} \right) \quad (3)$$

where $x = \hbar\omega_0/2k_bT$, Γ_0 is an anharmonic constant, and C is peak broadening related to phonon confinement and inhomogeneous strain. The parameters obtained from the fit of eq 3 to experimental data were as follows: $C = 4.39 \pm 0.1$ and $\Gamma_0 = 0.51 \pm 0.15$. Although the temperature dependence of the fwhm of the A_g² mode is visible, it is relatively small compared with other 2D materials such as MoS₂³⁵ for reasons that remain unclear. The change of the line width for A_g¹ and B_{2g} modes was less than the error of the fwhm determination (~0.5 cm⁻¹). Instead of the temperature dependence of the fwhm, we calculated the temperature dependence of their normalized intensity ratio. The intensity ratio of the Raman modes, as fwhm, is related to the phonon lifetime and their population;⁴¹ in our case, it allowed to reduce the effect of the error determination of the peak width. Figure 4b shows the calculated intensity of the A_g¹ and B_{2g} modes, normalized to the A_g² mode intensity. The intensity ratio of the B_{2g} mode to the A_g² mode increased by about 0.11 and the intensity ratio of the B_{2g} mode to the A_g² mode by about 0.22 when the temperature increased from 4 to 400 K. As can be noted, the intensity ratio of the B_{2g} mode to the A_g² mode is higher than that of the B_{2g} mode to the A_g² mode. We also observe that the intensity ratio increases with increasing temperature in a similar manner as the width of the A_g² mode. However, because the phonon properties of black phosphorus are still not fully understood, the explanation of this observation needs deeper theoretical insight, which is beyond the scope of this work.

CONCLUSIONS

In conclusion, we have investigated the temperature-dependent (temperature range 4–400 K) Raman spectra of few-layer black phosphorus flake supported on a SiO₂/Si substrate. In contrast to other works, a nonlinear dependence of the position of the three main Raman modes (A_g¹, B_{2g} and A_g²) was observed. The temperature dependence of the Raman mode position in the entire temperature range used was explained by the phenomenon of optical phonon decay into two or three acoustic phonons. At higher temperatures (above 250 K), the Raman mode position tended to linear dependence, and first-order temperature coefficients were calculated ($\chi = -0.0164$, -0.0271 , and -0.0283 cm⁻¹/K for A_g¹, B_{2g}, and A_g² modes, respectively). A nonlinear temperature dependence was also observed in the case of the fwhm of the A_g² mode and the intensity ratios of the A_g¹ and B_{2g} modes normalized to the A_g² mode. Our results can be used in further study of the thermal

properties of black phosphorus or the thermal metrology based on Raman spectroscopy^{13,42,43} of BP-based devices, which are still under development.

■ ASSOCIATED CONTENT

Supporting Information

The Supporting Information is available free of charge on the ACS Publications website at DOI: 10.1021/acs.jpcc.6b01468.

Details of error calculation; additional figures of AFM images (S1) and temperature dependence of Raman modes position (S2) of ~9.5 nm thick black phosphorus flake; parameters of fit to eqs 1 and 2 from main manuscript to experimental data (Tables S1 and S2) (PDF)

■ AUTHOR INFORMATION

Corresponding Author

*(M.Z.) E-mail: zdrojek@if.pw.edu.pl.

Present Address

[§]A.T. is also with the Institute of Electron Technology, Warsaw, Poland, and the Institute of Microelectronics and Optoelectronics, Warsaw University of Technology, Warsaw, Poland.

Author Contributions

^{||}A.Ł. and A.T. contributed equally.

Notes

The authors declare no competing financial interest.

■ ACKNOWLEDGMENTS

The work was supported by the Polish Ministry of Science and Higher Education within the Diamond Grant program (0025/DIA/2013/42). A.Ł. and J.J. thank the Polish National Science Centre for support within Project 2014/15/D/ST5/03944.

■ REFERENCES

- (1) Ling, X.; Wang, H.; Huang, S.; Xia, F.; Dresselhaus, M. S. The Renaissance of Black Phosphorus. *Proc. Natl. Acad. Sci. U. S. A.* **2015**, *112*, 4523–4530.
- (2) Qiao, J.; Kong, X.; Hu, Z.-X.; Yang, F.; Ji, W. High-Mobility Transport Anisotropy and Linear Dichroism in Few-Layer Black Phosphorus. *Nat. Commun.* **2014**, *5*, 5475.
- (3) Novoselov, K. S.; Jiang, D.; Schedin, F.; Booth, T. J.; Khotkevich, V. V.; Morozov, S. V.; Geim, A. K. Two-dimensional Atomic Crystals. *Proc. Natl. Acad. Sci. U. S. A.* **2005**, *102*, 10451–10453.
- (4) Liu, H.; Du, Y.; Deng, Y.; Ye, P. D. Semiconducting Black Phosphorus: Synthesis, Transport Properties and Electronic Applications. *Chem. Soc. Rev.* **2015**, *44*, 2732–2743.
- (5) Chen, X.; Wu, Y.; Wu, Z.; Han, Y.; Xu, S.; Wang, L.; Ye, W.; Han, T.; He, Y.; Cai, Y.; et al. High-Quality Sandwiched Black Phosphorus Heterostructure and its Quantum Oscillations. *Nat. Commun.* **2015**, *6*, 7315.
- (6) Gillgren, N.; Wickramaratne, D.; Shi, Y.; Espiritu, T.; Yang, J.; Hu, J.; Wei, J.; Liu, X.; Mao, Z.; Watanabe, K.; et al. Gate Tunable Quantum Oscillations in Air-Stable and High Mobility Few-Layer Phosphorene Heterostructures. *2D Mater.* **2015**, *2*, 011001.
- (7) Wang, H.; Wang, X.; Xia, F.; Wang, L.; Jiang, H.; Xia, Q.; Chin, M. L.; Dubey, M.; Han, S. Black Phosphorus Radio-Frequency Transistors. *Nano Lett.* **2014**, *14*, 6424–6429.
- (8) Na, J.; Lee, Y. T.; Lim, J. A.; Hwang, D. K.; Kim, G.-T.; Choi, W. K.; Song, Y.-W. Few-Layer Black Phosphorus Field-Effect Transistors with Reduced Current Fluctuation. *ACS Nano* **2014**, *8*, 11753–11762.
- (9) Li, L.; Yu, Y.; Ye, G. J.; Ge, Q.; Ou, X.; Wu, H.; Feng, D.; Chen, X. H.; Zhang, Y. Black Phosphorus Field-Effect Transistors. *Nat. Nanotechnol.* **2014**, *9*, 372–377.

(10) Haratipour, N.; Robbins, M. C.; Koester, S. J. Black Phosphorus p-MOSFETs With 7-nm HfO₂ Gate Dielectric and Low Contact Resistance. *IEEE Electron Device Lett.* **2015**, *36*, 411–413.

(11) Wu, J.; Mao, N.; Xie, L.; Xu, H.; Zhang, J. Identifying the Crystalline Orientation of Black Phosphorus Using Angle-Resolved Polarized Raman Spectroscopy. *Angew. Chem., Int. Ed.* **2015**, *54*, 2366–2369.

(12) Ribeiro, H. B.; Pimenta, M. A.; de Matos, C. J. S.; Moreira, R. L.; Rodin, A. S.; Zapata, J. D.; de Souza, E. A. T.; Castro Neto, A. H. Unusual Angular Dependence of the Raman Response in Black Phosphorus. *ACS Nano* **2015**, *9*, 4270–4276.

(13) Luo, Z.; Maassen, J.; Deng, Y.; Du, Y.; Garrelts, R. P.; Lundstrom, M. S.; Ye, P. D.; Xu, X. Anisotropic In-Plane Thermal Conductivity Observed in Few-Layer Black Phosphorus. *Nat. Commun.* **2015**, *6*, 8572.

(14) Late, D. J. Temperature Dependent Phonon Shifts in Few-Layer Black Phosphorus. *ACS Appl. Mater. Interfaces* **2015**, *7*, 5857–5862.

(15) Ong, Z.-Y.; Cai, Y.; Zhang, G.; Zhang, Y.-W. Strong Thermal Transport Anisotropy and Strain Modulation in Single-Layer Phosphorene. *J. Phys. Chem. C* **2014**, *118*, 25272–25277.

(16) Liu, H.; Neal, A. T.; Zhu, Z.; Luo, Z.; Xu, X.; Tománek, D.; Ye, P. D. Phosphorene: An Unexplored 2D Semiconductor with a High Hole Mobility. *ACS Nano* **2014**, *8*, 4033–4041.

(17) Srivastava, P.; Hembram, K. P. S. S.; Mizuseki, H.; Lee, K.-R.; Han, S. S.; Kim, S. Tuning the Electronic and Magnetic Properties of Phosphorene by Vacancies and Adatoms. *J. Phys. Chem. C* **2015**, *119*, 6530–6538.

(18) Li, Y.; Yang, S.; Li, J. Modulation of the Electronic Properties of Ultrathin Black Phosphorus by Strain and Electrical Field. *J. Phys. Chem. C* **2014**, *118*, 23970–23976.

(19) Erande, M. B.; Suryawanshi, S. R.; More, M. A.; Late, D. J. Electrochemically Exfoliated Black Phosphorus Nanosheets - Prospective Field Emitters: Electrochemically Exfoliated Black Phosphorus Nanosheets. *Eur. J. Inorg. Chem.* **2015**, *19*, 3102–3107.

(20) Late, D. J.; Liu, B.; Matte, H. S. S. R.; Rao, C. N. R.; Dravid, V. P. Rapid Characterization of Ultrathin Layers of Chalcogenides on SiO₂/Si Substrates. *Adv. Funct. Mater.* **2012**, *22*, 1894–1905.

(21) Sahoo, S.; Gaur, A. P. S.; Ahmadi, M.; Guinel, M. J.-F.; Katiyar, R. S. Temperature-Dependent Raman Studies and Thermal Conductivity of Few-Layer MoS₂. *J. Phys. Chem. C* **2013**, *117*, 9042–9047.

(22) He, M.; Rikkinen, E.; Zhu, Z.; Tian, Y.; Anisimov, A. S.; Jiang, H.; Nasibulin, A. G.; Kauppinen, E. I.; Niemelä, M.; Krause, A. O. I. Temperature Dependent Raman Spectra of Carbon Nanobuds. *J. Phys. Chem. C* **2010**, *114*, 13540–13545.

(23) Abdula, D.; Ozel, T.; Kang, K.; Cahill, D. G.; Shim, M. Environment-Induced Effects on the Temperature Dependence of Raman Spectra of Single-Layer Graphene. *J. Phys. Chem. C* **2008**, *112*, 20131–20134.

(24) Late, D. J.; Maitra, U.; Panchakarla, L. S.; Waghmare, U. V.; Rao, C. N. R. Temperature Effects on the Raman Spectra of Graphenes: Dependence on the Number of Layers and Doping. *J. Phys.: Condens. Matter* **2011**, *23*, 055303.

(25) Gaur, A. P. S.; Sahoo, S.; Scott, J. F.; Katiyar, R. S. Electron-Phonon Interaction and Double-Resonance Raman Studies in Monolayer WS₂. *J. Phys. Chem. C* **2015**, *119*, 5146–5151.

(26) Balandin, A. A. Thermal Properties of Graphene and Nanostructured Carbon Materials. *Nat. Mater.* **2011**, *10*, 569–581.

(27) Zhang, S.; Yang, J.; Xu, R.; Wang, F.; Li, W.; Ghufraan, M.; Zhang, Y.-W.; Yu, Z.; Zhang, G.; Qin, Q.; Lu, Y. Extraordinary Photoluminescence and Strong Temperature/Angle-Dependent Raman Responses in Few-Layer Phosphorene. *ACS Nano* **2014**, *8*, 9590–9596.

(28) Castellanos-Gomez, A.; Vicarelli, L.; Prada, E.; Island, J. O.; Narasimha-Acharya, K. L.; Blanter, S. I.; Groenendijk, D. J.; Buscema, M.; Steele, G. A.; Alvarez, J. V.; et al. Isolation and characterization of few-layer black phosphorus. *2D Mater.* **2014**, *1*, 025001.

(29) Novoselov, K. S.; Geim, A. K.; Morozov, S. V.; Jiang, D.; Zhang, Y.; Dubonos, S. V.; Grigorieva, I. V.; Firsov, A. A. Electric Field Effect in Atomically Thin Carbon Films. *Science* **2004**, *306*, 666–669.

(30) Island, J. O.; Steele, G. A.; van der Zant, H. S. J.; Castellanos-Gomez, A. Environmental Instability of Few-Layer Black Phosphorus. *2D Mater.* **2015**, *2*, 011002.

(31) Favron, A.; Gaufrès, E.; Fossard, F.; Phaneuf-L'Heureux, A.-L.; Tang, N. Y.-W.; Lévesque, P. L.; Loiseau, A.; Leonelli, R.; Francoeur, S.; Martel, R. Photooxidation and Quantum Confinement Effects in Exfoliated Black Phosphorus. *Nat. Mater.* **2015**, *14*, 826–832.

(32) Ling, X.; Liang, L.; Huang, S.; Piretzky, A. A.; Geohegan, D. B.; Sumpter, B. G.; Kong, J.; Meunier, V.; Dresselhaus, M. S. Low-Frequency Interlayer Breathing Modes in Few-Layer Black Phosphorus. *Nano Lett.* **2015**, *15*, 4080–4088.

(33) Jana, M. K.; Singh, A.; Late, D. J.; Rajamathi, C. R.; Biswas, K.; Felser, C.; Waghmare, U. V.; Rao, C. N. R. A Combined Experimental and Theoretical Study of the Structural, Electronic and Vibrational Properties of Bulk and Few-Layer Td-WTe₂. *J. Phys.: Condens. Matter* **2015**, *27*, 285401.

(34) Late, D. J.; Shirodkar, S. N.; Waghmare, U. V.; Dravid, V. P.; Rao, C. N. R. Thermal Expansion, Anharmonicity and Temperature-Dependent Raman Spectra of Single- and Few-Layer MoSe₂ and WSe₂. *ChemPhysChem* **2014**, *15*, 1592–1598.

(35) Pawbake, A. S.; Pawar, M. S.; Jadkar, S. R.; Late, D. J. Large Area Chemical Vapor Deposition of Monolayer Transition Metal Dichalcogenides and Their Temperature Dependent Raman Spectroscopy Studies. *Nanoscale* **2016**, *8*, 3008–3018.

(36) Yan, R.; Simpson, J. R.; Bertolazzi, S.; Brivio, J.; Watson, M.; Wu, X.; Kis, A.; Luo, T.; Hight Walker, A. R.; Xing, H. G. Thermal Conductivity of Monolayer Molybdenum Disulfide Obtained from Temperature-Dependent Raman Spectroscopy. *ACS Nano* **2014**, *8*, 986–993.

(37) Balkanski, M.; Wallis, R. F.; Haro, E. Anharmonic Effects in Light Scattering Due to Optical Phonons in Silicon. *Phys. Rev. B: Condens. Matter Mater. Phys.* **1983**, *28*, 1928–1934.

(38) Taube, A.; Judek, J.; Jastrzębski, C.; Duzynska, A.; Świtkowski, K.; Zdrojek, M. Temperature-Dependent Nonlinear Phonon Shifts in a Supported MoS₂ Monolayer. *ACS Appl. Mater. Interfaces* **2014**, *6*, 8959–8963.

(39) Taube, A.; Judek, J.; Łapińska, A.; Zdrojek, M. Temperature-Dependent Thermal Properties of Supported MoS₂ Monolayers. *ACS Appl. Mater. Interfaces* **2015**, *7*, 5061–5065.

(40) Dohčvić-Mitrović, Z. D.; Radović, M.; Šćpanović, M.; Grujić-Brojčin, M.; Popović, Z. V.; Matović, B.; Bošković, S. Temperature-Dependent Raman Study of Ce_{0.75}Nd_{0.25}O_{2-δ} Nanocrystals. *Appl. Phys. Lett.* **2007**, *91*, 203118.

(41) Shepherd, I. W. Temperature Dependence of Phonon Raman Scattering in FeBO₃, InBO₃, and VBO₃: Evidence for a Magnetic Contribution to the Intensities. *Phys. Rev. B* **1972**, *5*, 4524–4529.

(42) Taube, A.; Łapińska, A.; Judek, J.; Zdrojek, M. Temperature Dependence of Raman Shifts in Layered ReSe₂ and SnSe₂ Semiconductor Nanosheets. *Appl. Phys. Lett.* **2015**, *107*, 013105.

(43) Engel, M.; Steiner, M.; Han, S.-J.; Avouris, P. Power Dissipation and Electrical Breakdown in Black Phosphorus. *Nano Lett.* **2015**, *15*, 6785–6788.